Available online at www.sciencedirect.com

ScienceDirect

Ceramics International 35 (2009) 709–718

CERAMICS INTERNATIONAL

www.elsevier.com/locate/ceramint

Mechanical properties and cytotoxicity of 3Y-TZP bioceramics reinforced with Al_2O_3 particles

C. Santos [a,*], L.H.P. Teixeira [a], J.K.M.F. Daguano [a], S.O. Rogero [b], K. Strecker [c], C.N. Elias [d]

[a] *Universidade de São Paulo, Escola de Engenharia de Lorena/Departamento de Engenharia de Materiais, USP-EEL/DEMAR, Pólo Urbo-Industrial, Gleba AI-6 s/n, CEP 12600-000 Lorena, SP, Brazil*

[b] *Instituto de Pesquisas Energéticas e Nucleares, IPEN/CNEN-SP, Av. Prof. Lineu Prestes, CEP 05508-900, 2242 São Paulo, SP, Brazil*

[c] *Universidade Federal de São João del-Rei, Departamento de Mecânica, UFSJ-DEMEC, Campus Sto Antônio, Praça Frei Orlando 170, Centro, CEP 36.307-352, S.J. del-Rei, MG, Brazil*

[d] *Instituto Militar de Engenharia (IME), Pça. General Tibúrcio, 80 Praia Vermelha, CEP 22290-270, Rio de Janeiro, RJ, Brazil*

Received 5 April 2007; received in revised form 18 September 2007; accepted 4 February 2008

Available online 4 June 2008

Abstract

The influence of Al_2O_3 addition and sintering parameters on the mechanical properties and cytotoxicity of tetragonal ZrO_2–3 mol% Y_2O_3 ceramics was evaluated. Samples containing 0, 10, 20 and 30 wt.% of Al_2O_3 particles were prepared by cold uniaxial pressing (80 MPa) and sintered in air at 1500, 1550 and 1600 °C for 120 min. The effects of the sintering conditions on the microstructure were analyzed by X-ray diffraction analysis and scanning electron microscopy. Hardness and fracture toughness were determined by the Vickers indentation method and the mechanical resistance by four-point bending tests. As a preliminary biological evaluation, "in vitro" cytotoxicity tests were realized to determine the cytotoxic level of the ZrO_2–Al_2O_3 composites, using the neutral red uptake method with NCTC clones L929 from the American Type Culture Collection (ATCC) bank. Fully dense ceramic materials were obtained with a hardness ranging between 1340 HV and 1585 HV, depending on the amount of Al_2O_3 in the ZrO_2 matrix. On the other hand, no significant influence of the Al_2O_3 addition on fracture toughness was observed, exhibiting values near 8 MPa $m^{1/2}$ for all compositions and sintering conditions studied. The non-cytotoxic behavior, the elevated fracture toughness, the good bending strength ($\sigma_f = 690$ MPa) and the elevated Weibull's modulus ($m = 11$) exhibited by the material, show that these ceramic composites are highly suitable biomaterials for dental implant applications.

Keywords: A. Sintering; B. Microstructure-final; C. Mechanical properties; D. ZrO_2; D. Al_2O_3; E. Biomedical applications

1. Introduction

The development of technologies for the production of new biocompatible materials has been motivated by the demand for materials capable to support new specifications and applications [1,2]. The use of advanced ceramics as biomaterials started in the 1970s, and since then a continuous improvement of these materials in various application fields can be noted.

An important improvement has been possible by the use of ceramics as dental implant materials, because of their esthetic, biocompatibility and chemical inertness [1–3]. Currently, new dental implants based on high fracture toughness ceramics are developed, eliminating the metal support of the restorations with the objective to improve the esthetic aspects.

The most widely used ceramic biomaterials are alumina (Al_2O_3) and zirconia (ZrO_2) because of their excellent biocompatibility. The main advantages of Al_2O_3 are its high hardness and wear resistance, while ZrO_2 exhibits higher strength and fracture toughness, besides a lower Young's modulus [4–10].

It is a common knowledge that ZrO_2 additions may increase the fracture toughness of ceramic materials. This effect is based on the tetragonal to monoclinic phase-transformation of ZrO_2, accompanied with an increase of the specific volume in the order of 3–6% [5]. This volume increase generates stresses in the ceramic matrix, creating difficulties in crack propagation.

* Corresponding author. Tel.: +55 12 31599926; fax: +55 12 31533006.
E-mail address: claudinei@demar.eel.usp.br (C. Santos).

0272-8842/$34.00 © 2008 Elsevier Ltd and Techna Group S.r.l. All rights reserved.
doi:10.1016/j.ceramint.2008.02.004

Two composite materials are produced based on the ZrO_2–Al_2O_3 system: ATZ (alumina toughened zirconia) and ZTA (zirconia toughened alumina). In both cases, the fracture toughness of the ceramic matrix material is increased [4,11–14].

In vitro tests have been used to evaluate the biocompatibility of materials for over two decades, due to the easy availability of cell strains on the market [2]. The tests may not represent the real situation of an implant, but they provide results in a short period of time regarding the material's interactions in biological media, thus minimizing testing on live animals.

This work investigates the influence of sintering temperature, sintering time and Al_2O_3 content on the mechanical properties and cytotoxicity of ZrO_2–Al_2O_3 composites, with the objective to develop ceramic components for dental implants.

2. Experimental procedure

2.1. Processing

As starting powders, tetragonal ZrO_2, stabilized with 3 mol% Y_2O_3, containing 10% of residual monoclinic phase (designed TZ-3YSB, Tosoh Inc., Japan) and Al_2O_3 powder with an average particle size of 0.25 μm (SG-1000, Almatis, Alcoa-Group) were used. Four compositions were prepared varying the Al_2O_3 content in the ZrO_2 matrix from 0, 10, 20 to 30 wt.%.

The powder mixtures were prepared by attrition milling for 4 h in isopropyl alcohol, using ZrO_2 balls (2 mm diameter) as medium. After milling, the powder mixtures were dried at 90 °C for 24 h and deagglomerated. Specimens were obtained by cold uniaxial pressing under 80 MPa pressure.

Cylindrical samples of 15 mm diameter were sintered at 1500, 1550 and 1600 °C at 120 min. The heating rate varied according to the following program: 10 °C/min up to 1100 °C; 5 °C/min up to 1400 °C; and 3 °C/min until the final temperature. The cooling rate was 5 °C/min down to 1400 °C and 3 °C/min until the inertia of the furnace prevailed.

Samples containing 80 wt.% Al_2O_3 and 20 wt.% ZrO_2 were sintered in air at 1600 °C for up to 1440 min to evaluate the growth of the ZrO_2 and Al_2O_3.

2.2. Characterization

The particle size distribution of the powders after attrition milling was determined by sedigraph analysis. The shrinkage and weight loss during sintering of the composites were determined and the density was measured by the immersion method in distilled water, according to Archimedes' principle.

Crystalline phase analysis was done by X-ray diffractometry using Cu Kα radiation in the 2θ range of 20–80°, with a step width of 0.05° and 2 s of exposure time per position.

The average grain size of the ZrO_2 and Al_2O_3 phases was obtained by analyzing SEM images of polished and thermally etched surfaces (1300 °C, 15 min), with an image analyzer.

2.3. Mechanical properties

The mechanical properties, hardness and fracture toughness, were determined by Vickers indentations. For statistical reasons 21 indentations per sample were used, under a load of 20 N for 30 s. The fracture toughness has been calculated by the relation proposed by Evans and Charles [15], valid for Palmqvist cracks.

For the accomplishment of the bending tests, batches of 21 samples were grinded and polished, obtaining bars of 4 mm × 3 mm × 45 mm according to ASTM C 1116-94. The tests were conducted using a four-point bending device with outer and inner spans of 40 and 20 mm, respectively, as shown in Fig. 1, and a velocity of the crosshead displacement of 0.5 mm/s. The bending strength of the samples was calculated by

$$\sigma_f = \frac{3}{2} F_A \frac{I_1 - I_2}{bh^2} \quad (1)$$

where σ_f is the bending strength (MPa), F_A the rupture load (N), b the width of the samples (mm), h the height of the samples (mm), I_1 the outer span distance (mm) and I_2 is the inner span distance (mm).

For the statistical evaluation of the fracture strength the two-parameter Weibull distribution function has been used, according to

$$P = 1 - \exp\left\{\left[-\frac{\sigma}{\sigma_0}\right]^m\right\} \quad (2)$$

where P is the failure probability, m the Weibull's modulus, σ_0 the characteristic strength (MPa) and σ is the bending strength (MPa).

The Weibull's parameters m and σ_0, were obtained transforming Eq. (2) in Eq. (3) and plotting $\ln\ln[1/(1-P)]$ versus $\ln\sigma$.

$$\ln\ln\frac{1}{1/P} = m\ln\sigma - m\ln\sigma_0 \quad (3)$$

The stress value for 50% of rupture probability was estimated as reference and also for direct comparison with the average fracture stress. The Weibull's parameter "m" was determined using a factor of correction of 0.938, corresponding

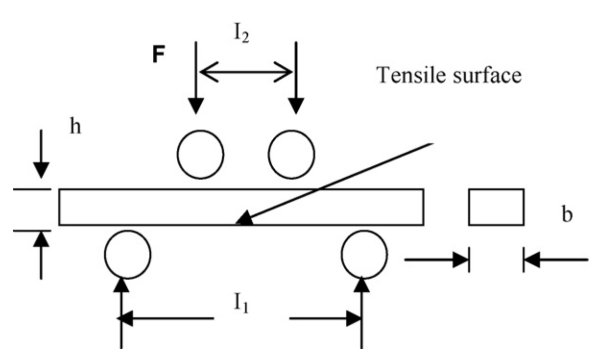

Fig. 1. Schematic illustration of the four-point bending test, with b the sample width (mm), h the sample height (mm), I_1 the outer span distance (mm) and I_2 the inner span distance (mm).

to 21 samples, in agreement with the German norm DIN-51-110.

2.4. Biocompatibility

The biocompatibility of the composites was evaluated by in vitro tests of the cytotoxicity CPCp, according to ISO 10993-part 5, by the neutral red uptake methodology [16,17].

2.4.1. Preparation of CPCp (ZrO_2:Al_2O_3 80:20) extracts

Samples of gamma sterilized CPCp were added to Eagle's minimum essential medium (MEM) in a proportion of 1 cm^2/mL and incubated for 48 h at 37 °C. Serial dilutions were made of extracts from the CPCp samples, the Al_2O_3 (negative control) and the 0.02% phenol solution (positive control).

2.4.2. Preparation of the cell suspension

The cell line NCTC clone L929 used was acquired from the American Type Culture Collection (ATCC) bank and were subcultured in MEM supplemented with 10% fetal calf serum, 20 mM glutamine and 1% non-essential amino acids (complete MEM), in a humidified incubator with 5% CO_2 at 37 °C. The cells were detached by trypsin, washed twice with calcium and magnesium free phosphate buffer solution and the cell suspension was adjusted to about 2.5×10^5 cells/mL.

2.4.3. Cytotoxicity assay

0.2 mL of the cell suspension was seeded in flat-bottomed 96 microplate wells (Costar, Cambridge, MA, USA). The microplate was incubated for 24 h at 37 °C in a CO_2 humidified incubator. After this period the medium of the plate was discarded and replaced with 0.2 mL of serially diluted extract of each sample (100, 50, 25, 12.5 and 6.25%). Control of the cell culture medium was replaced with complete MEM. In the same microplate, a positive (0.02% phenol solution) and negative control (high purity Al_2O_3) was run. Samples and controls were tested in triplicate. The plate was incubated again for 24 h under the same conditions.

After 24 h the culture medium and extracts were discarded and replaced with 0.2 mL of 0.005% neutral red diluted in MEM. After 3 h of incubation at 37 °C the dye medium was discarded and the microplate was washed twice with phosphate–saline buffer. The cells were washed with a solution of 1% $CaCl_2$ in 0.5% formaldehyde. The rupture of cells and neutral red release was obtained by adding 0.2 mL/well of extractant solution containing 50% ethanol in 1% acetic acid. The absorbances were read in a 540 nm filter on a RC Sunrise model—Tecan spectrophotometer for ELISA.

2.4.4. Cytotoxicity determination

With the average optical density of each extract dilution of samples, negative and positive controls of the cell viability percentage were calculated in relation to the cell control (100%) and plotted against the extract concentrations. The cytotoxicity of the investigated materials was expressed by a cytotoxicity index, $IC_{50(\%)}$, representing the concentration of the extract which injures or kills 50% of the cell population in the assay due to toxic elements extracted from the tested sample.

3. Results and discussion

3.1. Sintering

Fig. 2 presents the results of relative density as function of the sintering temperature and Al_2O_3 contents. Under all conditions, a small increase of the relative density was observed with increasing sintering temperature. Temperatures higher than 1500 °C resulted in relative densities higher than 99%, improving the mechanical properties and increasing the reliability, and, therefore, leading to materials with improved properties for structural applications.

It was noticed that the composites presented reduced and similar porosity levels, independent of the Al_2O_3 contents, thus the Al_2O_3 particles did not influence densification. This is justifiable because the powder mixtures had very close average particle sizes after attrition milling and, furthermore, the relative green density did not vary due to the Al_2O_3 additions, remaining constant at approximately 50%.

Fig. 3 presents the results of weight loss and linear shrinkage of the sintered samples, as a function of the Al_2O_3 content. It can be observed that the weight loss was very small in all cases

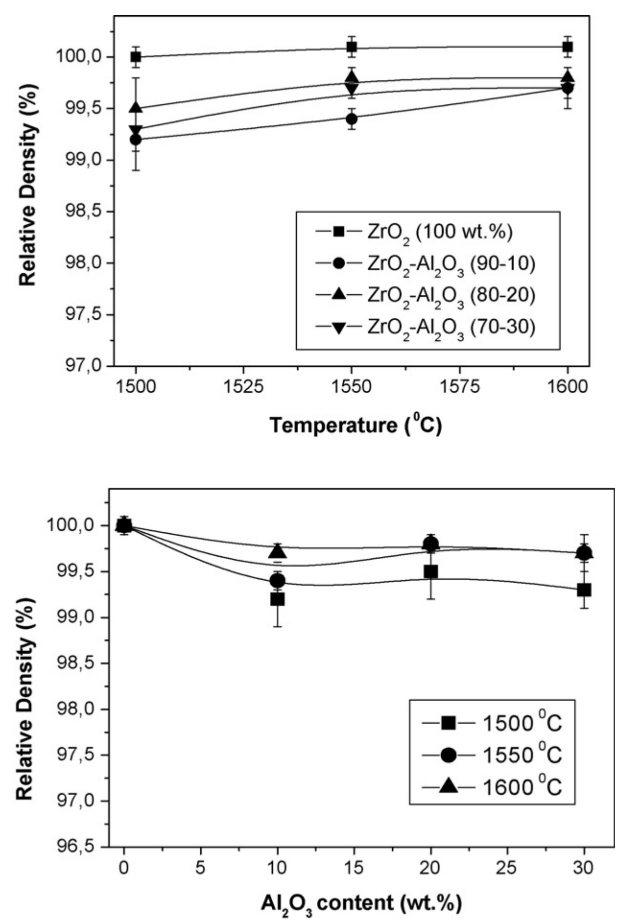

Fig. 2. Influence of the sintering temperature and Al_2O_3 content on the relative density of the sintered samples.

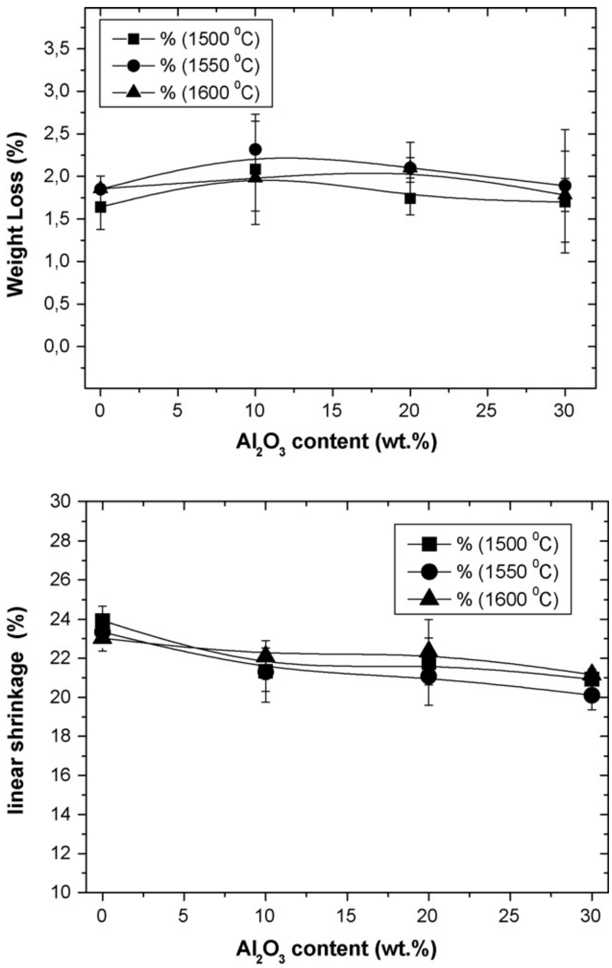

Fig. 3. Influence of Al_2O_3 content on weight loss and linear shrinkage of sintered samples.

and did not vary in regard of the sintering temperature or Al_2O_3 content added. The weight loss can be attributed to the volatilization of organic compounds used as lubricant during pressing.

Fig. 4 presents X-ray diffraction patterns of different samples sintered at 1600 °C. Similar patterns were obtained for composites sintered at 1500 and 1550 °C. In all materials sintered only the tetragonal ZrO_2 phase has been observed, showing that the monoclinic ZrO_2 phase content in the starting-powder has been completely transformed, and indicating the complete stabilization of the tetragonal phase during cooling. The presence of Al_2O_3 phase had no influence on the phase-transformation rates during the sintering process. The increasing Al_2O_3 peak intensities are due to increasing amounts in the ZrO_2 matrix.

It is known [5] that the application of compressive stresses on a tetragonal ZrO_2 surface, such as induced during grinding and polishing procedures, may trigger the tetragonal–monoclinic phase-transformation, T–M. Fig. 5 presents X-ray diffractogram patterns of ZrO_2–Al_2O_3 surfaces after grinding and polishing samples sintered at 1500 °C and 1600 °C for 120 min. As can be observed no monoclinic-ZrO_2 is present as characterized by diffraction peaks at $2\theta = 28^\circ$ and 31°. Therefore, it can be deduced that no T–M transformation has not occurred, or that the amount transformed is lower than 2 vol%, which is the detection limit of the diffractometer.

Based on the results of the mechanical properties of the ZrO_2–Al_2O_3 composites, samples with composition 80 wt.% ZrO_2–20 wt.% Al_2O_3, were sintered at 1600 °C, with isothermal sintering times varying between 0 and 1440 min to study the influence of sintering time on microstructure and mechanical properties. The results indicate insignificant differences in relative density, weight loss, linear shrinkage or crystalline phases, while hardness and fracture strength decreases slightly (see below).

3.2. Microstructure

3.2.1. Effect of Al_2O_3 additions

Fig. 6 presents micrographs of the ZrO_2–Al_2O_3 composites with varying Al_2O_3 contents sintered at 1600 ° in 120 min. The presence of the two distinct phases, ZrO_2 (clear phase) and

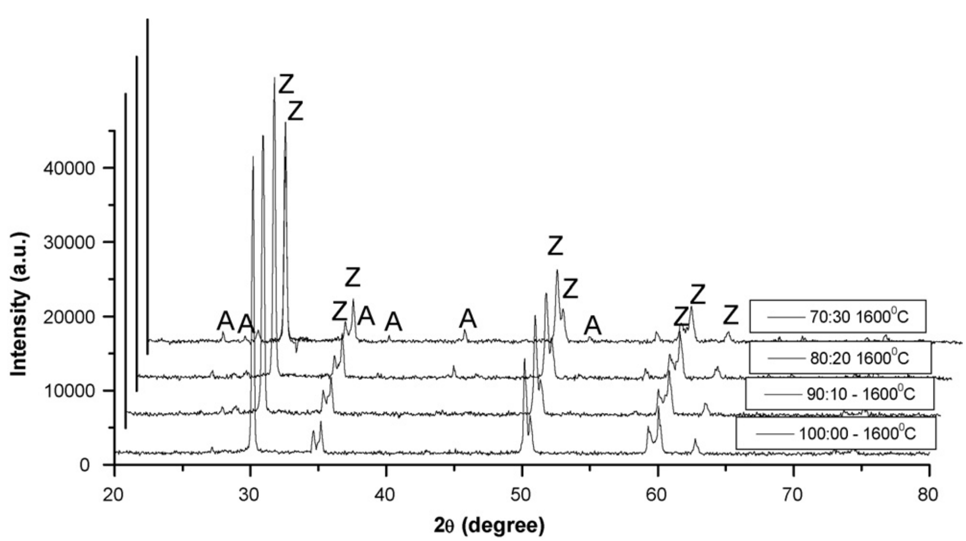

Fig. 4. X-ray diffraction patterns of the ZrO_2–Al_2O_3 composites, sintered at 1600 °C.

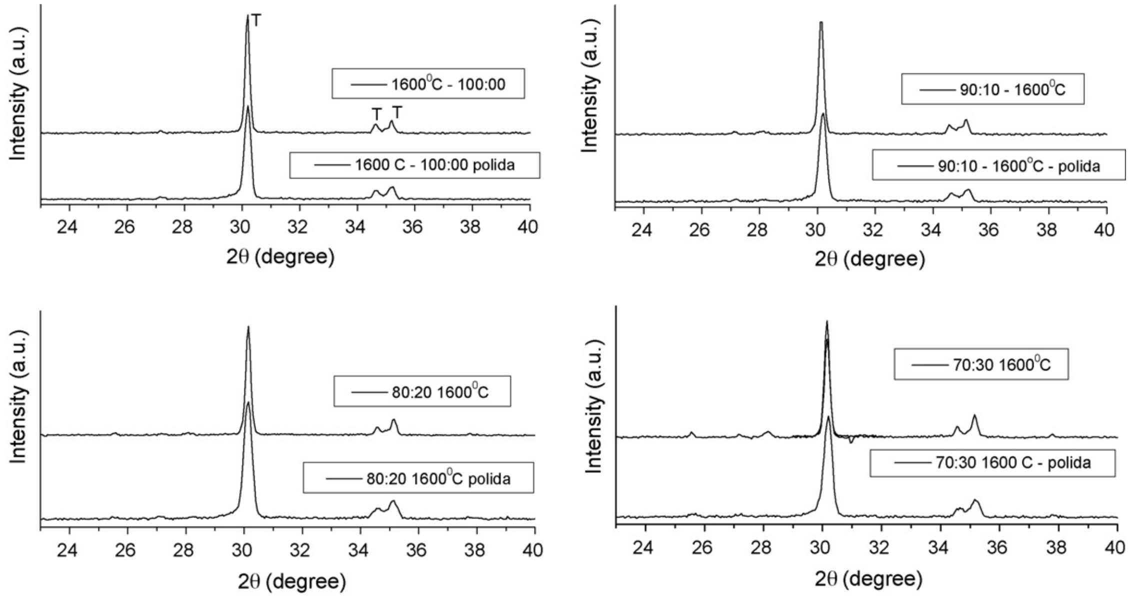

Fig. 5. X-ray diffraction patterns of polished surfaces of samples, with different Al_2O_3 contents sintered at 1600 °C.

Al_2O_3 (dark phase) can be clearly seen, as well as an increasing amount of Al_2O_3 grains due to increasing Al_2O_3 contents in the composite materials.

Table 1 summarizes the microstructural parameters grain density and grain size of the ZrO_2–Al_2O_3 composites. With increasing amounts of Al_2O_3 larger grain sizes of both phases, Al_2O_3 and ZrO_2, are observed. The different inclination of the curves of the average grain sizes of the ZrO_2 and Al_2O_3 phases in function of the Al_2O_3 content, see Fig. 7, indicate different grain growth rates. It can be observed that the grain growth rate of the Al_2O_3 phase is higher than that of the ZrO_2 phase.

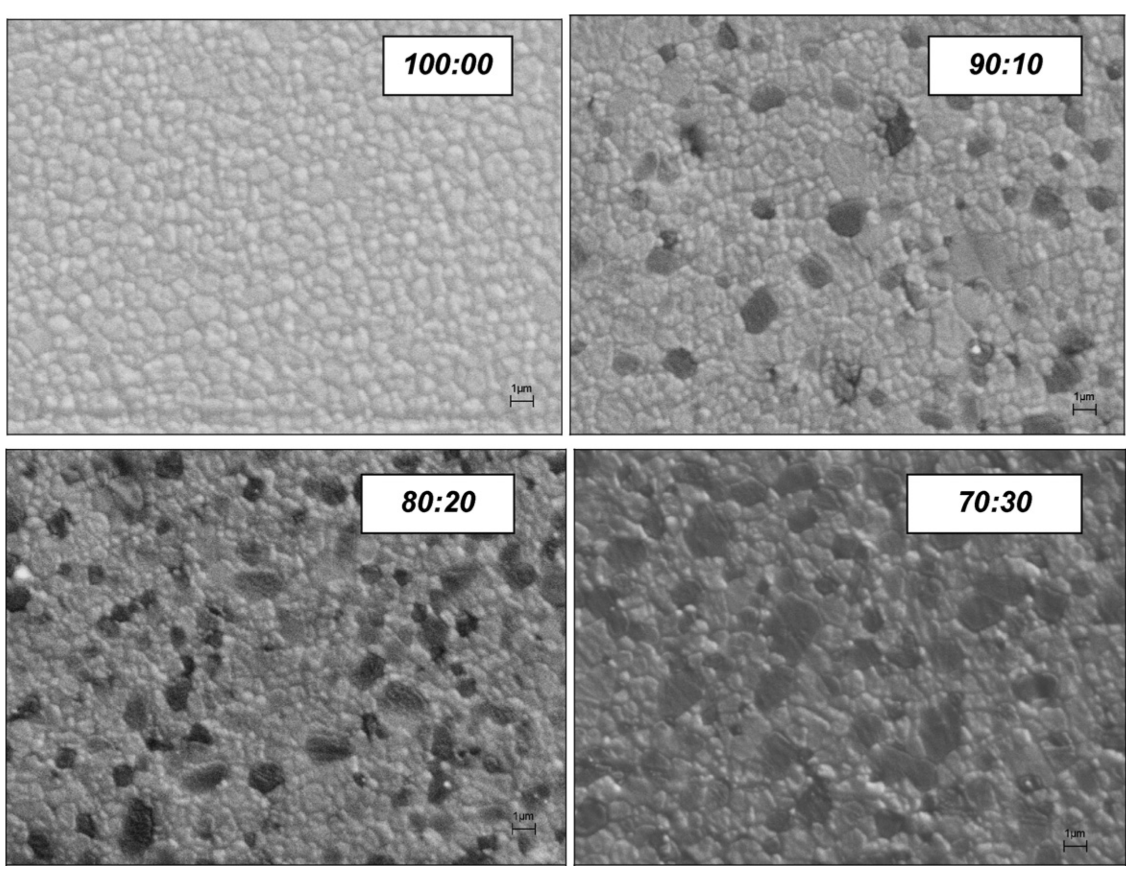

Fig. 6. Micrographs of the ZrO_2–Al_2O_3 composites sintered at 1600 °C, for different Al_2O_3 contents (magnification, 8000×).

Table 1
Microstructural parameters of the ZrO_2–Al_2O_3 composites, sintered at 1600 °C

Composition ZrO_2–Al_2O_3	Grain density (grains/μm^2)	Average grain size (μm)
70–30		
Al_2O_3	0.18	1.67 ± 0.38
ZrO_2	1.07	0.65 ± 0.12
80–20		
Al_2O_3	0.15	1.29 ± 0.27
ZrO_2	1.51	0.53 ± 0.14
90–10		
Al_2O_3	0.13	0.77 ± 0.18
ZrO_2	2.02	0.50 ± 0.11
100–00		
ZrO_2	2.08	0.48 ± 0.09

3.2.2. *Effect of sintering time*

In Fig. 8 SEM micrographs of the same samples sintered at 1600 °C for different times are shown. Furthermore, Fig. 9 presents the average grain sizes of the ZrO_2 and Al_2O_3 phases in relation with the isothermal sintering time. Grain growth of both phases, Al_2O_3 and ZrO_2, can be clearly noted as sintering time increases. A similar behavior has been observed by Alexander et al. [18], for Al_2O_3–ZrO_2 composites.

3.2.3. *Kinetics of grain growth*

The grain growth during sintering can be described by [19,20]:

$$G^n - G_0^n = Kt \quad (4)$$

where G represents the grain size at time t, G_0 is the initial grain size at $t = 0$, K a constant which depends on the temperature and the activation energy of grain growth and n is the grain growth exponent, characteristic of the growth mechanism.

The grain growth exponent n is represented by the inclination of the straight line obtained by linear regression of the logarithmic graph *grain size* versus *time* (see Fig. 10). The results are also listed in Table 2. The grain growth exponent, n, for the ZrO_2 and Al_2O_3 phase were 2.8 and 4.1, respectively, indicating that different mechanisms are responsible for the grain growth of each phase. A growth exponent of $n = 4$ indicates a grain boundary diffusion controlled process, while an exponent of $n = 3$ indicates a volume diffusion controlled process. The grain growth exponents for the ZrO_2 and Al_2O_3 found in this work are in agreement with the works of Alexander et al. [18].

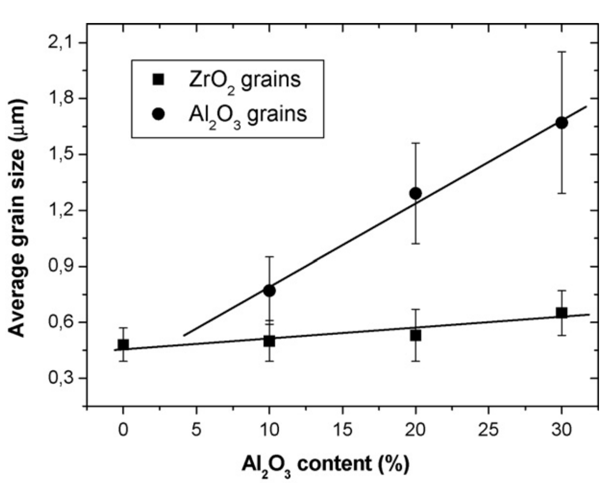

Fig. 7. Average grain size as function of the Al_2O_3 content.

3.3. *Mechanical properties*

3.3.1. *Hardness and fracture toughness*

The results of Vickers hardness and fracture toughness of samples sintered at different temperatures are presented in Fig. 11, as function of the Al_2O_3 content and the sintering temperature.

It can be observed from Fig. 2 that under all temperatures, a relative density higher than 99% has been achieved, so that decreasing porosity did not cause the increase of hardness of the composites as shown in Fig. 11. This increase is attributed to the Al_2O_3 additions causing a linear increase in hardness, reaching values ranging between 1350 and 1600 HV for an addition of 0 and 30% of Al_2O_3, respectively, representing a 20% increase of hardness by adding 30% of Al_2O_3. Furthermore, the small standard deviation indicate an elevated homogeneity of the samples. In previous works, similar hardness results were obtained in ZTP–Al_2O_3 composites, with hardness varying between 12 and 16 GPa [21,22].

Fracture toughness has not been affected by the Al_2O_3 addition in ZrO_2 matrix. In this case, besides the martensitic transformation of the ZrO_2 phase, the thermal residual stress generated by the incorporation of the Al_2O_3 particles, which present a different coefficient of thermal expansion (CTE) as the ZrO_2 matrix, contribute to the high fracture toughness, varying between 7.8 and 8.2 MPa $m^{1/2}$. This mechanism was also related by Nawa et al. [21], in Ce–TZP–30% Al_2O_3 composites development.

Based on the high hardness and fracture toughness, samples containing 20 wt.% of Al_2O_3 were sintered at 1600 °C, for various times. Fig. 12 presents the effect of the sintering time on the hardness and fracture toughness. With the increasing sintering time, a slight reduction of hardness and fracture toughness of the sintered ZrO_2–Al_2O_3 composites was observed. This observation is attributed to the increasing grain size, reducing the number of grains per area and causing a smaller degree of crack deflection by the grain boundaries.

3.3.2. *Bending strength and failure probability*

Samples containing 20 wt.% of Al_2O_3 and sintered at 1600 °C for 120 min presented a bending strength close to 690 MPa, Young's modulus of 200 GPa and a fracture toughness of 8 MPa $m^{1/2}$. Commercial *In-Ceram zirconia*® is considered as one of the commercial dental ceramics that present better mechanical properties. This material, which is composed of incorporated glass-infiltrated Al_2O_3–3Y-TZP ceramics is obtained by *slip casting* technique and present a

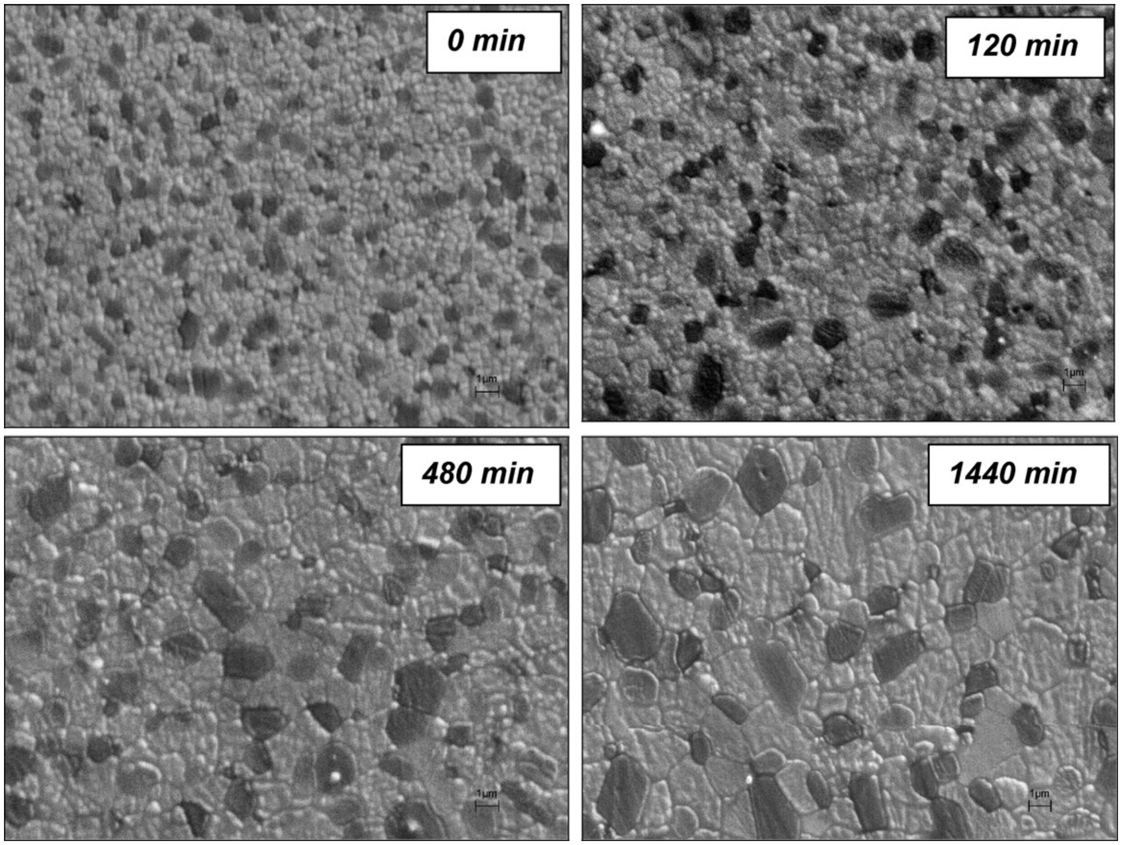

Fig. 8. Micrographs of the 80:20 ZrO_2–Al_2O_3 composite sintered at 1600 °C for different times.

Young's modulus of 260 GPa, bending strength of 600 MPa and fracture toughness near to 4.4 MPa $m^{1/2}$. Despite the different obtaining process and the composition, the absolute values obtained in this paper indicate that this ceramic, obtained by a simple processing technique, present better mechanical properties than commercial material.

Fig. 13 presents results of the failure probability and the Weibull diagram of samples of composition 80% of ZrO_2 and 20% of Al_2O_3 sintered at 1600 °C for 120 min. Usually, the Weibull parameter, *m*, strongly depends on processing, microstructure, pore distribution and surface finishing degree. For common ceramic materials *m*-values between 3 and 15 have been determined. According to Quinn [23], ceramic materials with *m* higher than 10 may be considered good and reliable, and are suitable for structural applications. A Weibull modulus of 11.7 has been determined for the ZrO_2–Al_2O_3 80:20 samples, which permits its application as dental material due to the high reliability.

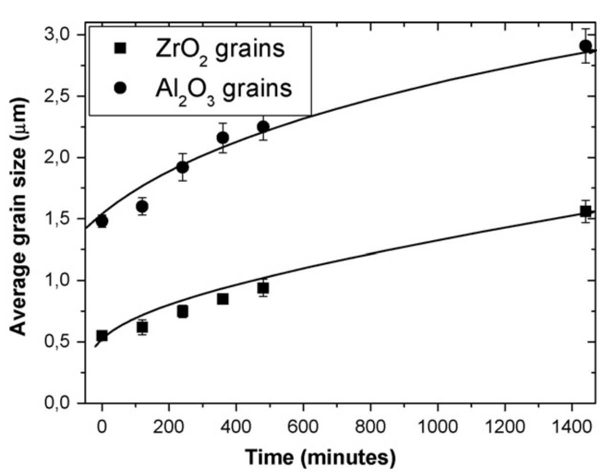

Fig. 9. Average grain sizes of the ZrO_2 and Al_2O_3 phases of the composite sintered at 1600 °C for different times.

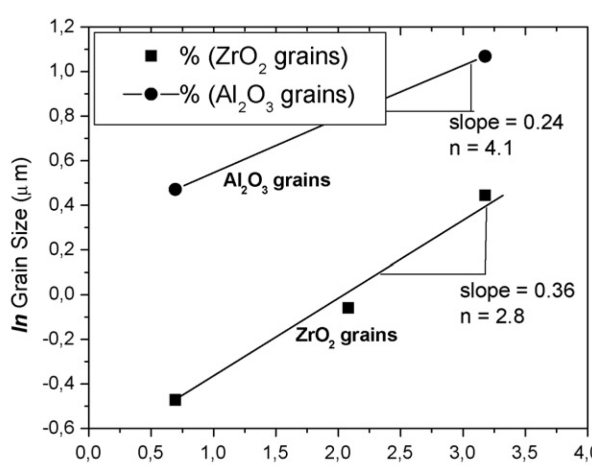

Fig. 10. Grain sizes of the ZrO_2 and Al_2O_3 phases versus sintering time.

Table 2
Linear regression results of the microstructural parameters

Sintering time (min)	Grain size average (μm)	ln grain size	Linear regression
ZrO_2			
120	0.62 ± 0.06	−0.471	$Y = -0.75418 + 0.36566x$ (correlation coefficient = 0.992)
480	0.94 ± 0.07	−0.060	
1440	1.56 ± 0.09	0.444	
Al_2O_3			
120	1.60 ± 0.08	0.471	$Y = 0.30607 + 0.2405x$ (correlation coefficient = 0.998)
480	2.25 ± 0.11	0.809	
1440	2.91 ± 0.14	1.068	

3.4. Biological evaluation

The evaluation of the biological compatibility of the ZrO_2–Al_2O_3 composites was done by the incorporation of the ''Neutral Red'', in the cytoplasm and lysosomal membranes of living cells, which were in contact with the ceramic material.

By plotting the average percentage of cell survival in function of the extract concentration, the cytotoxicity index ($CI_{50\%}$) is obtained, corresponding to the concentration where 50% of cells survived. It is known, that the negative control simulates an environment where the cell has total capacity of development and to create colonies, while the positive control simulates an environment totally adverse to its development. Fig. 14 shows the results obtained for the composites sintered at 1600 °C and of the controls used. This analysis showed promising results, because the viability of 90% of the composite material is clearly above the 80% viability limit, which indicates an excellent biocompatibility of the material. Therefore, it can be affirmed that the ZrO_2–Al_2O_3 composite material obtained in this work can be classified as non-cytotoxic, therefore having great potential for possible applications as implants.

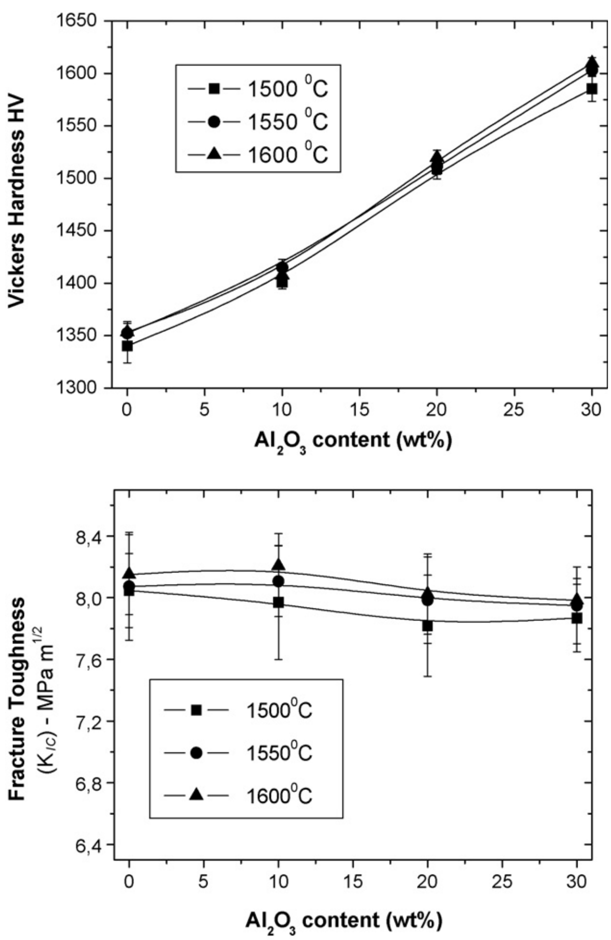

Fig. 11. Influence of sintering time and Al_2O_3 content on the hardness and fracture toughness of the sintered samples.

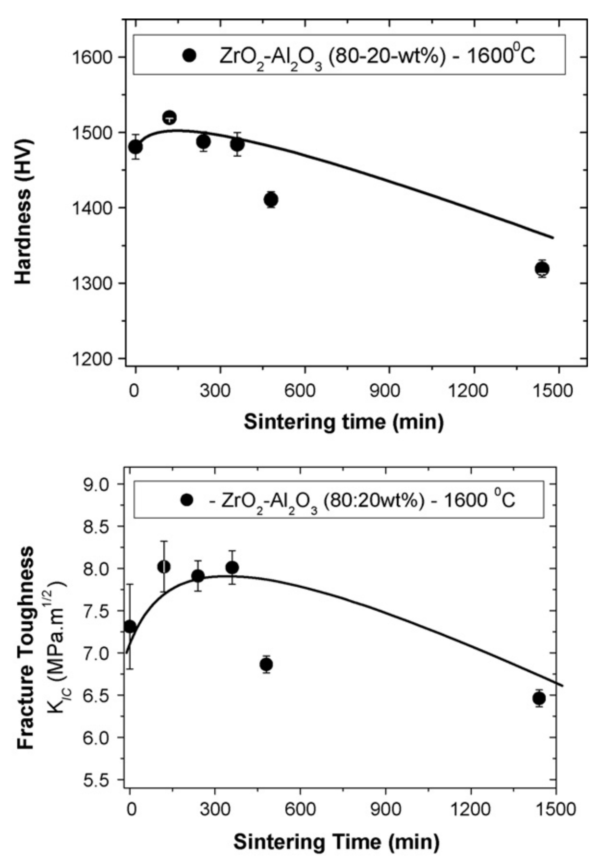

Fig. 12. Vickers hardness and fracture toughness of the sintered composites versus time.

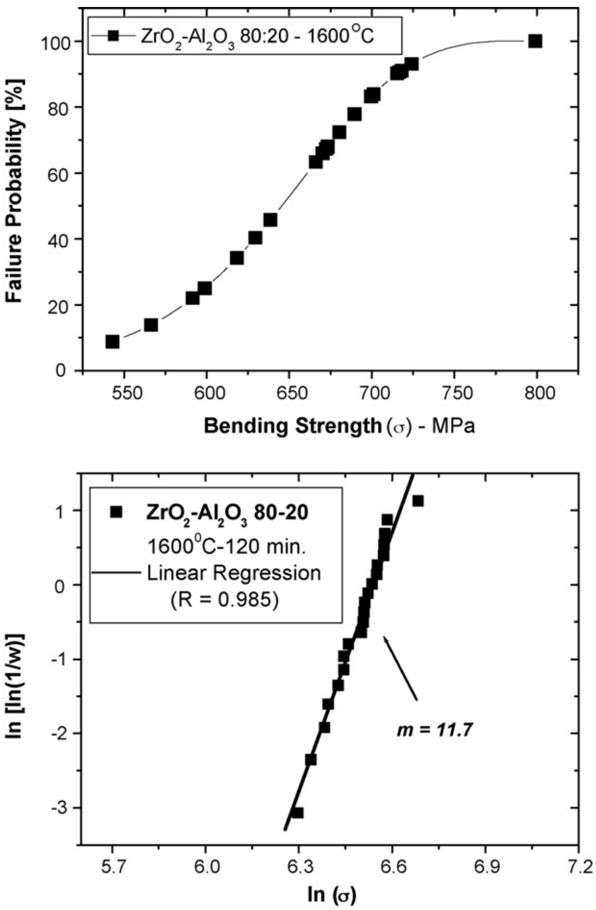

Fig. 13. Failure probability and Weibull diagram of the ZrO_2–Al_2O_3 composites sintered at 1600 °C, for 120 min.

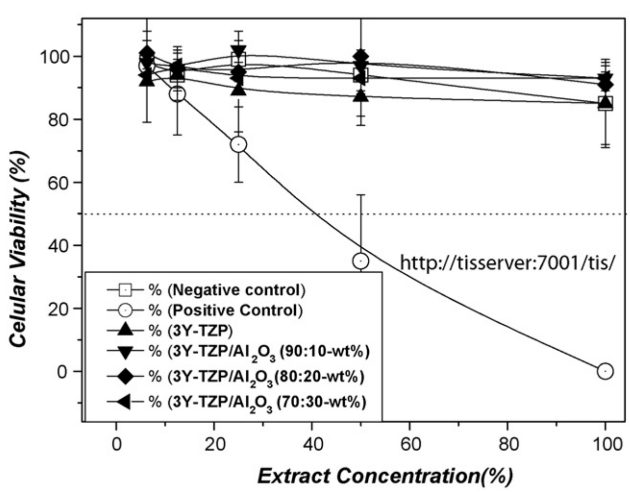

Fig. 14. Viability curves of sintered ZrO_2–Al_2O_3 composite ceramics in the cytotoxicity test by neutral red uptake assay.

4. Conclusions

Highly dense ZrO_2–Al_2O_3 composites were obtained when sintered at temperatures higher than 1500 °C. In all sintered materials only the tetragonal ZrO_2 phase has been observed, indicating the complete stabilization of the tetragonal phase during cooling. Al_2O_3 had no influence on the phase-transformation, but influenced the grain growth of both phases, Al_2O_3 and ZrO_2. It has been observed that the grain growth rate of the Al_2O_3 phase is higher than that of the ZrO_2 phase. The grain growth exponent, n, for the ZrO_2 and Al_2O_3 phase were 2.8 and 4.1, respectively, indicating a volume diffusion controlled process for ZrO_2 and a grain boundary diffusion controlled process for Al_2O_3. A linear increase in hardness of the composite materials with increasing amounts of Al_2O_3 has been observed; for an addition of 30% of Al_2O_3 hardness reached 1600 HV. On the other hand, the fracture toughness of about 8 MPa $m^{1/2}$ of the composites has not been affected by the Al_2O_3 content. Apparently, lower t-ZrO_2 contents are compensated by stresses generated by the thermal mismatch between the ZrO_2 matrix and the Al_2O_3 grains.

The bending strength of samples containing 20 wt.% of Al_2O_3 sintered at 1600 °C for 120 min, was close to 690 MPa, besides a Young's modulus of 200 GPa. Furthermore, the preliminary testing of the biocompatibility showed that the ZrO_2–Al_2O_3 composite material can be classified as non-cytotoxic, therefore having great potential for possible applications as implant components. It has been shown in this work that ZrO_2–Al_2O_3 composite may be used as bioceramic material in applications such as dental implants due to its excellent mechanical properties and biocompatibility, besides its esthetic.

Acknowledgements

The authors would like to thank *FAPESP* for financial support, under Grant no. 04/04386-1 and the students Renata Hage Amaral and Jeniffer Borges Asnal from *IPEN-CNEN/SP* for technical assistance and Resolina Pereira dos Santos from *Instituto Adolfo Lutz* for preparation of the cell cultures.

References

[1] L.L. Hench, Bioceramics, J. Am. Ceram. Soc. 81 (7) (1998) 1705–1728.
[2] D.F. Willians, Biofunctionality and biocompatibility, in: Medical and Dental Materials, VCH, New York, 1992.
[3] L.L. Hench, J. Wilson, An Introduction to Bioceramic, vol. 1, World Scientific, Singapura, 1993, pp. 1–3 (Adv. Ser. Ceram., 1).
[4] A.H. De Aza, J. Chevalier, G. Fantozzi, et al., Crack growth resistance of alumina, zirconia and zirconia toughened alumina ceramics for joint prostheses, Biomaterials 23 (2002) 937–945.
[5] R. Stevens, An Introduction to Zirconia: Zirconia and Zirconia Ceramics, 2nd ed., Magnesium elektrum, Twickenham, 1986 (Magnesium Elektron Publications, n113).
[6] D. Basu, B.K. Sarkar, Toughness determination of zirconia toughened alumina ceramics from growth of indentation-induced cracks, J. Mater. Res. 11 (12) (1996) 3057–3062.
[7] B. Basu, J. Vleugels, O. Van Der Biest, ZrO_2–Al_2O_3 composites with tailored toughness, J. Alloys Compd. 365 (1–2) (2004) 266–270.
[8] C. Piconi, G. Maccauro, Zirconia as a ceramic biomaterial, Biomaterials 20 (1999) 1–25.
[9] C. Piconi, W. Burger, H.G. Richter, A. Cittadini, G. Maccauro, V. Covacci, N. Bruzzese, G.A. Ricci, E. Marmo, Y-TZP ceramics for artificial joint replacements, Biomaterials 19 (16) (1998) 1489–1494.
[10] R. Stevens, Zirconia: second phase particle transformation toughening of ceramics, Trans. Br. Ceram. 80 (1981) 81–85.

[11] M. Rühle, A. Stecker, D. Waidelich, B. Kraus, In situ observations of stress-induced phase transformation in ZrO_2 containing ceramics, in: N. Claussen, M. Rülle, A. Heuer (Eds.), Advanced in Ceramics. Science and Technology II, vol. 12, American Ceramic Society, Columbus, 1984, pp. 256–274.

[12] B.L. Karihaloo, Contributions of T–M phase transformation to the toughening of ZTA, J. Am. Ceram. Soc. 74 (1991) 1703–1706.

[13] P.F. Becher, K.B. Alexander, W. Warmick, Influence of ZrO_2 grain size and content on the transformation response in the Al_2O_3–ZrO_2(12% mol CeO_2) system, J. Am. Ceram. Soc. 76 (1993) 657–663.

[14] G. Gregori, W. Burger, V. Sergo, Piezo-spectroscopic analysis of the residual stress in zirconia-toughened alumina ceramics: the influence of the tetragonal-to-monoclinic transformation, Mater. Sci. Eng. A 271 (1999) 401–406.

[15] A.G. Evans, E.A. Charles, Fracture toughness determination by indentation, J. Am. Ceram. Soc. 59 (10) (1976) 7–8.

[16] International Organization for Standardization, Biological Evaluation of Medical Devices. Part 1. Guidance on Selection of Tests, 1993, p. 29 (ISO 10993-1).

[17] International Organization for Standardization, Biological Evaluation of Medical Devices. Part 5. Tests for Cytotoxicity: In Vitro Methods, 1993 (ISO 10993-5).

[18] K.B. Alexander, P.F. Becher, S.B. Waters, A. Bleier, Grain growth kinetics in alumina–zirconia (CeZTA) composites, J. Am. Ceram. Soc. 77 (4) (1994) 939–946.

[19] R. Oberacker, F. Thummler, An Introduction to Powder Metallurgy, The Institute of Materials, 1993,, p. 332.

[20] R.M. German, Sintering Theory and Practice, John Wiley and Sons, 1996, p. 550.

[21] M. Nawa, S. Nakamoto, T. Sekino, K. Niihara, Tough and strong Ce–TZP/alumina nanocomposites doped with titania, Ceram. Int. 24 (7) (1998) 497–506.

[22] Y. Ye, J. Li, H. Zhou, J. Chen, Microstructure and mechanical properties of yttria-stabilized ZrO_2/Al_2O_3 nanocomposite ceramics, Ceram. Int. 34 (2008) 1797–1803.

[23] G.D. Quinn, Strength and proff testing, Engineered Materials Handbook, vol. 4, Ceramics and Glasses, ASM International, Metals Park, OH, 1991, pp. 585–598.